Taylor & Francis
Taylor & Francis Group

Combustion Science and Technology

ISSN: 0010-2202 (Print) 1563-521X (Online) Journal homepage: www.tandfonline.com/journals/gcst20

Impact of Detailed Molecular Transport on Ammonia/Hydrogen Ignition Delay Time Measurements in Rapid Compression Machines

Chunwei Wu, Robert Schießl & Ulrich Maas

To cite this article: Chunwei Wu, Robert Schießl & Ulrich Maas (10 Apr 2026): Impact of Detailed Molecular Transport on Ammonia/Hydrogen Ignition Delay Time Measurements in Rapid Compression Machines, Combustion Science and Technology, DOI: 10.1080/00102202.2026.2654683

To link to this article: https://doi.org/10.1080/00102202.2026.2654683

Published online: 10 Apr 2026.

COMBUSTION SCIENCE AND TECHNOLOGY
https://doi.org/10.1080/00102202.2026.2654683

Impact of Detailed Molecular Transport on Ammonia/Hydrogen Ignition Delay Time Measurements in Rapid Compression Machines

Chunwei Wu, Robert Schießl, and Ulrich Maas

Institute of Technical Thermodynamic, Karlsruhe Institute of Technology, Karlsruhe, Germany

ABSTRACT

The influence of detailed molecular transport, notably, of thermo-diffusion, in the compressed fuel/air mixture in rapid compression machine experiments is studied by detailed numerical simulations. The evolution of a one-dimensional layer of fuel-air mixture subjected to an RCM process was simulated using detailed treatment of transport and chemical reaction. The simulation includes compression work and wall heat losses as essential RCM processes, and adds a detailed treatment of molecular transport processes and chemical reaction within the gas mixture to the description. The model outcome reveals how detailed transport can create inhomogeneities in the initially homogeneous mixture composition, well before chemical reaction sets in. The effect is pronounced in hydrogen-containing mixtures, where temperature gradients at the near-wall boundary layer can cause notable "un-mixing" of hydrogen by thermo-diffusion. This can effectively lead to inhomogeneous fuel-air ratio fields, which are present already when the RCM compression phase is finished. Under these circumstances, the ignition delay and temperature assigned to a RCM experiment correspond to a physically different auto-ignition event than nominal. Neglecting these effects may lead to a bias in reported experimental ignition delay time curves.

ARTICLE HISTORY
Received 7 November 2025
Revised 9 January 2026
Accepted 16 January 2026

KEYWORDS
Rapid compression machine; numerical simulation; thermo-diffusion; molecular transport

Introduction

Hydrogen (H_2) and ammonia (NH_3) are both promising zero – carbon fuels, and interest in their use has been increasing in recent years. Hydrogen exhibits high reactivity, which is advantageous for ignition and flame propagation, but its large-scale use is constrained by limited availability and safety concerns (Cavalcanti et al. 2024; Huang 2024). Ammonia, on the other hand, is readily available and easier to store, but its low reactivity limits combustion performance (Drost et al. 2023). Fuel blending provides a practical approach to combine their complementary advantages, enhancing ignition and combustion characteristics while maintaining a low-carbon footprint (Huang 2024). These considerations motivate the present study on ammonia – hydrogen ignition delay characteristics.

The dependence of ignition delay time (IDT) on pressure and temperature is an important characteristic of any fuel. For the case of ammonia(NH_3)/hydrogen(H_2)

CONTACT Chunwei Wu chunwei.wu@kit.edu

mixtures, there is a paucity of ignition delay time measurements. This contrasts with the importance of these mixtures as prospective carbon-free fuels. More experimental IDT data for these substances are desired, in order to improve the kinetic models and, therefore, the predictivity of combustion models.

IDTs can be measured in Rapid Compression Machines (RCM, see e.g. (Sung and Curran 2014)).Many researchers have extensively used RCMs to measure ignition delay times of a wide range of fuels, including hydrocarbons, hydrogen, and ammonia-related mixtures (Donohoe et al. 2014; Goyal et al. 2018; He et al. 2019). These studies have established RCMs as a robust platform for high-accuracy IDT determination and kinetic model validation across pressures, temperatures, and equivalence ratios relevant to practical combustion systems.

However, accurately reproducing experimentally measured IDT by kinetic mechanisms under varying conditions remains a significant challenge (Alnasif et al. 2023). Simulations of the auto-ignition in RCMs often rely on homogeneous reactor models, which do not account for factors like in-cylinder flow and heat transfer to the cold wall, which affect the ignition process observed in experiments (Grogan et al. 2015). Classify the relative influence of these factors to form a regime diagram characterizing RCM experiments.

Beyond homogeneous reactor surrogates, a major strand of RCM modeling has focused on physics-based multi-zone heat-loss models (MZM) that relax the adiabatic assumption while retaining computational efficiency. In particular, Goldsborough and coworkers formulated an MZM that partitions the reaction chamber and explicitly accounts for conductive losses in the core, convective losses in the piston crevice, and blow-by through the ring pack, and showed that such losses can be coupled to the adiabatic-core model for improved IDT prediction (Goldsborough et al. 2012). Subsequent applications and extensions have demonstrated good agreement with multi-dimensional RCM simulations and experiments (Goldsborough et al. 2013; Sung and Curran 2014; Wilson and Allen 2017). However, by construction these reduced-order MZM formulations assume each zone to be compositionally homogeneous; they do not resolve multicomponent species diffusion or thermo-diffusion (Soret effect) driven by temperature gradients. These mass transfer by diffusion can be an important influence on the auto-ignition process. For instance, in hydrogen-containing mixtures, the low molar mass and high diffusivity of H_2 (see e.g. (Giacomazzi et al. 2023)) can cause an "un-mixing" of hydrogen at temperature gradients by thermo-diffusion. This can effectively result in a stratified fuel-air ratio field, and thus affect ignition behavior.

In addition to physics-based RCM models, recent studies have explored data-driven approaches, such as ANN-based surrogate modeling combined with Bayesian inference, to optimize kinetic parameters against extensive ignition datasets (Liao et al. 2023). While effective for parameter calibration and uncertainty quantification, such approaches do not replace physics-based models that are required to elucidate transport effects and boundary-layer phenomena in RCM experiments.

In previous studies, the importance of accounting for diffusion effects in hydrogen/ammonia ignition in rapid compression machines (RCMs) was mainly discussed in the context of turbulent conditions (see, e.g., Li et al. (2024); Pan et al. (2020)). However, even in the most fundamental laminar RCM auto-ignition configurations, the formation of a thermal boundary layer may induce local un-mixing and species stratification, which can in turn influence the predicted ignition delay time. The present work focuses on this

aspect and aims to clarify the role of transport modeling and boundary-layer-induced diffusion effects on ignition delay predictions under laminar RCM conditions.

To assess the influence of thermo-diffusion, a one-dimensional model is employed to model auto-ignition in a system that evolves under detailed chemical kinetics and detailed molecular transport. The model simulates a laminar layer of fuel/air mixture which extends from the center of the chamber to the wall. We used detailed transport model to show the effect of differential diffusion and thermo-diffusion on the ignition. Results show that effects of detailed transport can notably alter the mixture before and during the induction phase, so that conditions at ignition can deviate from those in the initial compressed mixture. These alterations can become notable within the typical time scales of ignition delay in RCM experiments (say, several 10 ms), and their neglect may lead to a bias in reported experimental ignition delay time curves.

Methodology

The impact of detailed molecular transport on the auto-ignition during a typical RCM experiment is studied by numerical simulations of species- and temperature profiles in a laminar layer of the reacting gas mixture in the RCM-chamber. Attention is given to full spatial and temporal resolution. In particular, the interplay of detailed molecular transport processes (transport of energy by heat conduction and species diffusion, transport of chemical species by diffusion and by thermo-diffusion, regarding different diffusivities among species and between mass and energy) with detailed chemical kinetics is modeled.

This is achieved with the in-house code INSFLA (Maas and Warnatz 1988), which solves the detailed equations for reaction and molecular transport for a reacting ideal-gas mixture on a 1D region. The code applies automatic grid adaption and time stepping with error control on the solution. The simulated region is a line in the center of the RCM chamber, spanning the axial distance from the piston surface to the cylinder head (Figure 1).

The numerical treatment uses the Lagrangian coordinate ψ and the time t as independent variables, where ψ is defined via

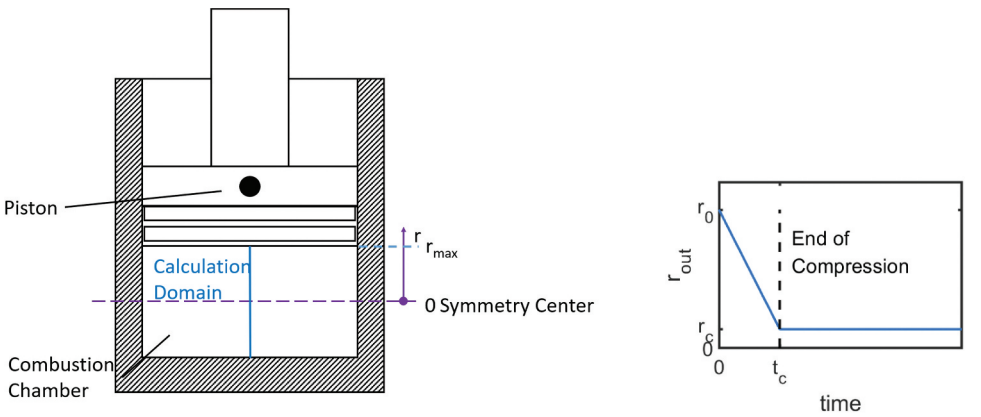

Figure 1. Left: location of the calculation domain within the RCM combustion chamber. Right: shape of the compression curve (motion of the outer boundary). The values t_c, r_0 and r_c can be varied.

$$\frac{\partial \psi}{\partial r} = \rho r^{\alpha}$$

with the spatial coordinate r, the state-dependent gas density ρ and the geometry-dependent parameter α. For an infinite slab, as is used in this study, $\alpha = 0$; for infinite cylinder, $\alpha = 1$ and for a sphere, $\alpha = 2$. The infinite slab geometry is chosen because the axial length scale is much smaller than the radial dimension towards the end of compression and after compression, resulting in an approximately planar geometry with dominant axial gradients while radial variations can be neglected. Using ψ instead of the spatial coordinate r as independent variable in the model allows easily incorporating moving boundaries. This is useful in RCM modeling, when the compression process induced by the moving piston is to be modeled.

The equations solved for the dependent variables spatial coordinate $r(t, \psi)$, temperature $T(t, \psi)$, pressure $p(t, \psi)$ and mass fractions of the n_s chemical species $w_i(t, \psi)$ $(i = 1, \ldots, n_s)$ read (Maas and Warnatz 1988):

$$\begin{aligned}
&\tfrac{\partial r}{\partial \psi} - \tfrac{1}{\rho r^{\alpha}} = 0 \\
&\tfrac{\partial p}{\partial \psi} = 0 \\
&\tfrac{\partial T}{\partial t} - \tfrac{1}{\rho c_p}\tfrac{\partial p}{\partial t} - \tfrac{1}{c_p}\tfrac{\partial}{\partial \psi}\left(\rho r^{\alpha}\lambda \tfrac{\partial T}{\partial \psi}\right) + \tfrac{1}{\rho c_p}\sum_{i=1}^{n_s} \omega_i h_i M_i + \\
&\tfrac{r^{\alpha}}{c_p}\sum_{i=1}^{n_s} \rho w_i V_i c_{pi}\tfrac{\partial T}{\partial \psi} = 0 \\
&\tfrac{\partial w_i}{\partial t} + \tfrac{\partial}{\partial \psi}\left(\rho r^{\alpha} w_i V_i\right) - \tfrac{\omega_i M_i}{\rho} = 0
\end{aligned} \tag{1}$$

Here, c_p, λ are the specific isobaric heat capacity and thermal conductivity of the gas mixture, respectively. The indexed variables $\omega_i, M_i, h_i, w_i, x_i, c_{p\,i}$ and V_i denote the chemical source term, molar mass, specific enthalpy, mass fraction, mole fraction, specific isobaric heat capacity and difussion velocity, respectively, of species i. Complemented with the ideal gas equation of state

$$p = \rho R T,$$

this is a system of $n_s + 3$ equations in the $n_s + 3$ coordinate- and time-dependent fields w, p, r, t.

In planar geometry, $a = 0$. The total diffusive mass flux of species i is taken as the sum of Fickian diffusion and thermo-diffusion (Soret effect):

$$j_i(\psi) = j_i^D + j_i^T = -\rho D_i \frac{\partial w_i}{\partial \psi} - \rho D_i^T \frac{1}{T}\frac{\partial T}{\partial \psi}$$

where D_i is the mass diffusivity and D_i^T is the thermal diffusion coefficient. By definition, the total mass flux of species i is

$$j_i = \rho w_i V_i$$

The equation system then reads:

$$
\begin{aligned}
&\frac{\partial r}{\partial \psi} - \frac{1}{\rho} = 0 \\
&\frac{\partial p}{\partial \psi} = 0 \\
&\frac{\partial T}{\partial t} - \frac{1}{\rho c_p}\frac{\partial p}{\partial t} - \frac{1}{c_p}\frac{\partial}{\partial \psi}\left(\rho\lambda\frac{\partial T}{\partial \psi}\right) + \frac{1}{\rho c_p}\sum_{i=1}^{n_s}\omega_i h_i M_i - \\
&\frac{1}{c_p}\sum_{i=1}^{n_s}\rho\left(\rho D_i \frac{w_i}{x_i}\frac{\partial x_i}{\partial \psi} + \frac{D_i^T}{T}\frac{\partial T}{\partial \psi}\right)c_{pi}\frac{\partial T}{\partial \psi} = 0 \\
&\frac{\partial w_i}{\partial t} - \frac{\partial}{\partial \psi}\left(\rho\left[\rho D_i \frac{w_i}{x_i}\frac{\partial x_i}{\partial \psi} + \frac{D_i^T}{T}\frac{\partial T}{\partial \psi}\right]\right) - \frac{\omega_i M_i}{\rho} = 0
\end{aligned}
\tag{2}
$$

For future studies with different geometries (cylindrical, spherical), only the value of α has to be modified.

The source terms ω_i are evaluated using the detailed reaction mechanism for ammonia/hydrogen from Shrestha et al. (Shrestha et al. 2018). This chemical mechanism consists of 34 species and 278 elementary reactions and has been validated against experimental ignition delay time data for ammonia (see e.g. Kawka et al. (2020)). Owing to its demonstrated predictive capability, it has been frequently used in numerical investigations of ammonia combustion (see e.g. Wu et al. (2024); D'Antuono et al. (2024)).

The one-dimensional simulation domain can qualitatively describe the impact of molecular transport on the ignition delay time (IDT).

The simulation starts with initially homogeneous fields for all variables, corresponding to cold, uncompressed, unreacted mixture. The RCM compression process is modeled using a time-dependent boundary condition for the coordinate of the outer boundary according to a prescribed function $r_{\text{out}} = \tilde{r}(t)$. The motion causes r_{out} to fall from r_0 at $t = 0$ to a lower value r_c at $t = t_c$ (compression duration). After this, the motion ceases and the system remains isochoric. The motion of the outer boundary transfers compression work to the system, thus causing temperature and pressure to rise. The imposed boundary motion curve was prescribed to represent a typical rapid compression machine (RCM) compression process and to achieve the target end-of-compression conditions relevant to the present study.

Initially (at time $t = 0$), all fields (species and temperature) are homogeneous. The initial conditions consisted of homogeneous fuel/air mixtures with an initial temperature T_c. In this study, stoichiometric mixtures containing 40 % NH_3 and 60 % H_2 were investigated.

The inner boundary ($\psi = 0$) is treated as a symmetry center, with Dirichlet boundary condition $r = 0$, and Neumann boundary conditions with zero gradient for all other dependent variables.

The outer boundary is positioned at the cold wall. The Dirichlet boundary condition $T_w = 376$ K is imposed to the outer boundary on the temperature, maintaining an isothermal wall. The species boundary condition taken from an isotherm, inert wall is

$$j_i = j_i^M + j_i^T = 0,$$

where j_i^M denotes the mass flux of species caused by concentration gradients (i.e., by Fickian diffusion) and j_i^T denotes the mass flux of species caused by temperature gradient (i.e., by thermo-diffusion). A moving outer boundary is achieved by imposing a time-dependent Dirichlet boundary condition on the spatial coordinate r, $r(t, \psi_{out}) = r_{out}(t)$. The initial and boundary conditions are summarized in Table 1.

Table 1. Initial and boundary conditions used in the one-dimensional simulations.

Location	Variable	Condition
Initial condition ($t = 0$)	Species mass fractions Y_i	Homogeneous, stoichiometric mixture of $40\%NH_3/60\%H_2$/air
	Temperature T	$T = T_c$
	Pressure p	$p = p_c$
Inner boundary ($\psi = 0$)	Radial coordinate r	$r = 0$ (symmetry center)
	Species mass fractions Y_i	$\frac{\partial Y_i}{\partial \psi} = 0$
	Temperature T	$\frac{\partial T}{\partial \psi} = 0$
	Pressure p	$\frac{\partial p}{\partial \psi} = 0$
Outer boundary ($\psi = \psi_{out}$)	Radial coordinate r	$r(t, \psi_{out}) = r_{out}(t)$
	Species mass flux j_i	$j_i = j_i^M + j_i^T = 0$
	Temperature T	$T = T_w = 376$K (isothermal wall)
	Pressure p	$\frac{\partial p}{\partial \psi} = 0$

In 1-D simulations using INSFLA, detailed molecular transport was applied. Diffusion caused by concentration gradient is modeled using a reduced Stefan – Maxwell formulation with effective mixture-averaged diffusion coefficients derived from binary diffusivities (Hirschfelder et al. 1964; Bird et al. 2002; Warnatz et al. 2006). Thermo-diffusion (Soret effect) is accounted for by an additional temperature-gradient – driven flux term using the Paul – Warnatz formulation (Paul and Warnatz 1998).

One-dimensional axial formulation is used here, which is physically justified by the much smaller axial length scale compared to the radial dimension after compression. While radial temperature gradients may still exist due to wall heat loss close to the cylinder liner, their magnitude is negligible compared to the dominant axial temperature gradient. Although some 3-D effects are not accounted for with 1-D simulations, they provide an efficient way to study the influence of thermo-diffusion on the auto-ignition process.

Figure 2 shows exemplary results of these simulations; for simplicity, the source terms were turned off in this instance. The simulation begins with a flat temperature profile at $t = 0$. The inwards-moving outer boundary causes the domain to shrink and, consequently, the gas to be compressed. This raises the temperature in the domain; at the outer boundary, the boundary condition forces low temperature throughout all timesteps. Compression ends after $t = 50\,ms$. After this, the temperature decreases by heat losses.

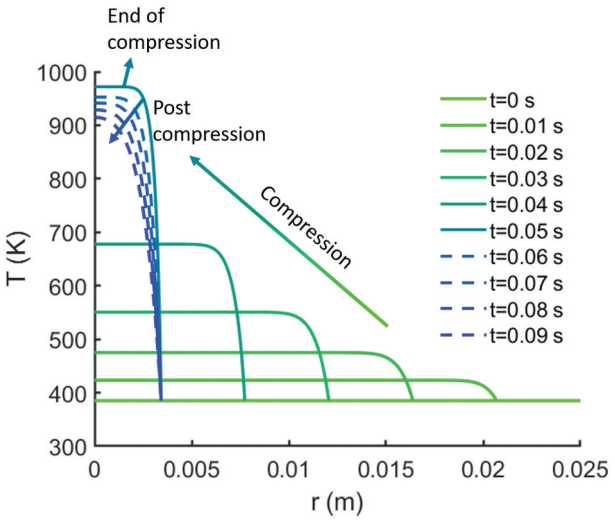

Figure 2. Evolution of temperature during and after compression in the 1D model.

Analysis of the simulated RCM process

The simulated data (notably, T_c, p_c and the resulting pressure trace $p(t)$) are used like experimental RCM data as the basis for a data evaluation procedure to obtain ignition delay time and the temperature and pressure associated with an ignition event.

Moreover, 0-D homogeneous reactor simulations of the ignition event are performed to investigate the impact of detailed molecular transport. Firstly, inert 1-D simulations were performed to obtain the inert pressure trace $p(t)$ corresponding to inert gas measurements in RCM experiments. Then, under the isentropic assumption, the volume trace $v(t)$ was calculated from the conservation equations and the ideal gas law. The volume trace $v(t)$ was then used as the input for homogeneous reactor simulations. For details of the simulations with adiabatic core assumption, see e.g (Drost et al. 2023).

In both 1-D simulations and homogeneous reactor simulations, detailed chemical kinetics with the mechanism for NH_3 and H_2 developed by Shrestha et al. were applied (Shrestha et al. 2018). The ignition delay time (IDT) in both simulations was defined as the duration from $t = 0$ to the point where the pressure gradient reaches its maximum, which is aligned with experimental conventions.

Results and discussion

Results

Non-reacting case. First, a non-reacting $40\%NH_3/60\%H_2$ (mol/mol)/air at $\phi = 1$, $T_c = 960$ K, $p_c = 15$ bar was simulated. To achieve this, the chemical reactions were "shut off," so that only molecular transport processes affect the system. Figure 3 shows the resulting profiles of species mole fractions, temperature, and equivalence ratio after 40 ms. The equivalence ratio was calculated using the H/O atom ratio: $\phi = \frac{w_H/w_O}{(w_H/w_O)_{\text{stoich.}}}$. Due to the boundary effect, which is the heat transfer to the cold wall, a thermal boundary layer at the outer boundary (formed by the cylinder top) has formed. The temperature gradient at

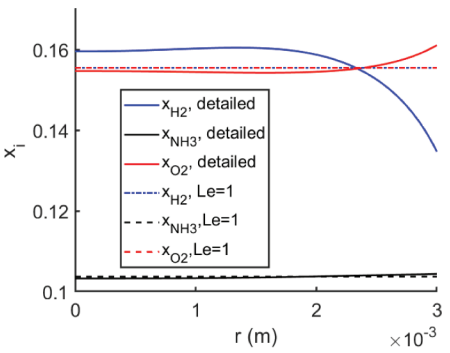

(a) Mole fractions of H_2, NH_3 and O_2, showing effects of thermal diffusion

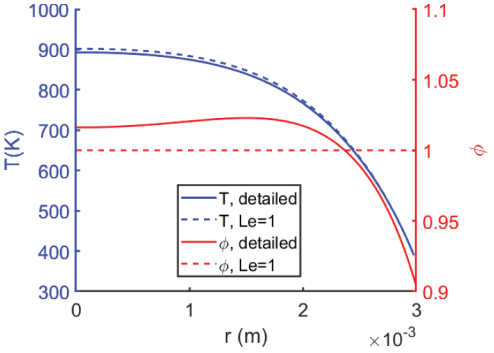

(b) Temperature and equivalence ratio showing the effect of heat conduction and differential diffusion

Figure 3. Temperature and species profiles for non-reacting mixture of $40\%NH_3$ / $60\%H_2$ / air at $\phi = 1$, $T_c = 960$ K, $p_c = 15$ bar, $t = 40$ ms, $r_{max} = 3$ mm. Results from the detailed transport model (solid lines) are compared to a simplified transport model assuming a Lewis number of unity (Le = 1, dotted lines).

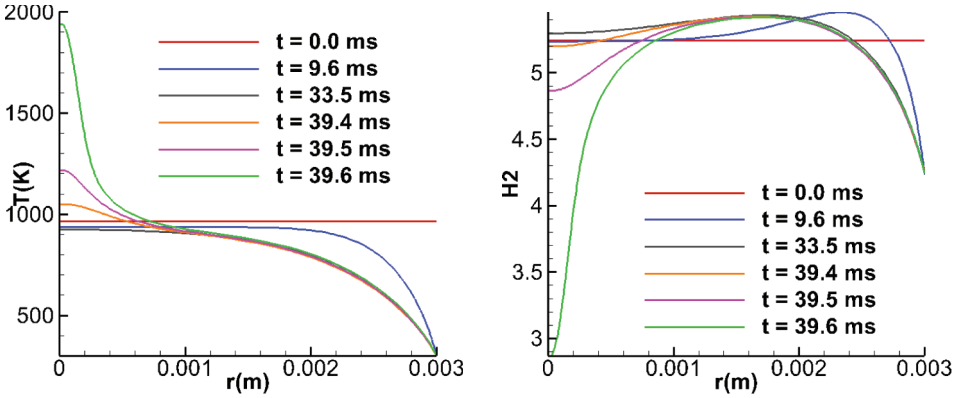

(a) Temperature profile showing auto-ignition in the middle of the calculation domain

(b) H_2 mass fraction showing the reaction and diffusion of hydrogen

Figure 4. Spatio-temporal evolution of temperature and hydrogen concentration for the auto-ignition of mixture of 40%NH_3 / 60%H_2 / air at $\phi = 1$, $T_c = 960$ K, $p_c = 15$ bar.

this thermal boundary layer wall causes diffusion of species by thermo-diffusion. Figure 3 shows this effect, both for simulations with a detailed transport model (solid lines) and for simulations with equal species diffusivity and a unity Lewis number assumption (dotted lines). In the simplified transport model, the diffusion coefficient D for all species is assumed to be identical and is calculated from the thermal conductivity λ to ensure Le = 1. The simplified Le = 1 case is used purely for comparison purposes to highlight the effect of detailed transport; it does not correspond to the stoichiometric equivalence ratio of the mixture. Since the diffusivity of hydrogen is larger than that of ammonia, H_2 diffuses faster into the high-temperature region in the detailed transport model. The differential diffusion, therefore, causes an un-mixing of the initially homogeneous gas mixture, resulting in a space-dependent equivalence ratio. At the outer boundary, the temperature is lower, and the mixture is "leaner" compared to the center.

Reacting case. To further demonstrate the effect of molecular transport on the auto-ignition process and to estimate the IDT using the 1D model, the simulation was repeated with chemical reactions included. Figure 4 shows the spatio-temporal evolution of temperature and hydrogen concentration for the auto-ignition in a 40%NH_3 / 60%H_2 / air mixture at $\phi = 1$, $T_c = 960$ K, $p_c = 15$ bar. During the ignition delay period, a temperature gradient caused by heat conduction to the cold wall and thermo-diffusion of hydrogen into the high-temperature zone can be observed, like in the inert case. Starting at approximately 30 ms, auto-ignition begins to occur. However, unlike in the homogeneous reactor, where auto-ignition occurs simultaneously throughout the entire domain, the temperature rise and auto-ignition in the 1D case initiate in a localized region at the center, while the rest of the mixture remains unignited. Later, as the flame propagates, all mixtures will be burned.

Discussion

The detailed molecular transport affects the auto-ignition process in several ways.

Differential diffusion alters the equivalence ratio ϕ (mainly due to the different diffusion behavior of H_2 and O_2). It also alters the molar ratio r of the fuel components ($r = H_2/NH_3$). Both effects are notable even in the center of the domain (Figure 4). Figure 5(a) shows the temporal evolution of ϕ and r for one condition. Results for both detailed and simplified transport are shown. This can lead to an assignment of a measured ignition event (and its ignition delay time) in an RCM to physically incorrect values of ϕ and r. The deviation between the nominal and actual values first increases with the time after compression. This is due to the buildup of the "unmixing process" by the different diffusivities of the components in the fuel/air mixture. The deviation then decreases again; this is consistent with the "leveling-out" of the compositional inhomogeneities (which were temporarily created by different diffusivities) on longer timescales. In the example of Figure 5, the maximum deviation (in the order of 5% for both ϕ and r) is seen near 100 ms after compression. At different conditions (especially, for lean mixtures), one can expect even larger deviations, and also different time scales of the deviations' buildup and decay.

Comparable trends were also observed with a 50% NH_2 /50% H_2 mixture, indicating the robustness of the results.

As described in Sec. 3, the IDT was calculated using both 1-D simulations and homogeneous reactor simulations, with the IDT defined as the duration from $t = 0$ to the point where the pressure gradient reaches its maximum.

The ignition delay time data for a stoichiometric mixture of $60\%NH_3/40\%H_2$ at 10 bar are shown in Figure 6. While the physical conditions under which the auto-ignition event occurs are affected by detailed transport, the ignition delay time as such is affected only little in the example studied here. This is because near $\phi = 1$, the ignition delay time is not very sensitive with respect to changes in ϕ, and also not with respect to changes in the NH_3/H_2 ratio r near $r = 0.6/0.4$. Therefore, the evaluation procedure which assigns a temperature and pressure to an ignition event is hardly affected by detailed transport any more than it is

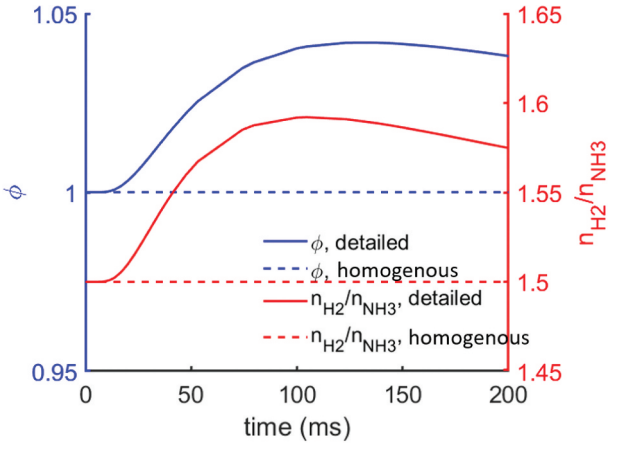

Figure 5. Temporal evolution of equivalence ratio and H_2/NH_3 ratio in the center of the domain, as a function of time. Data for a mixture affected by detailed transport (solid lines) and for a homogeneous mixture, (which results when detailed transport is ignored) are shown.

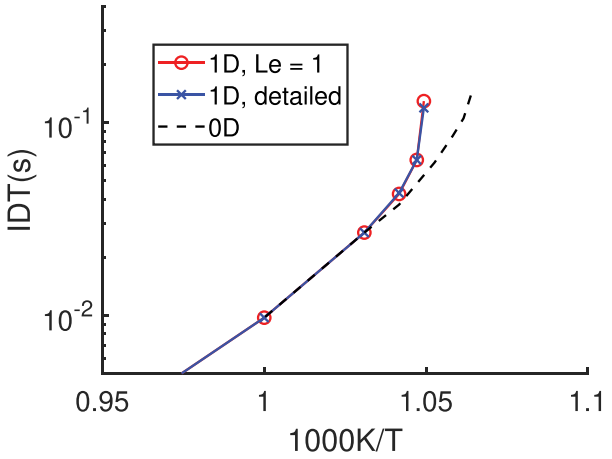

Figure 6. Dependence of the ignition delay time of a stoichiometric mixture of 60%NH_3/40%H_2 on temperature at 15 bar, obtained from homogeneous reactor simulations (dashed line), one-dimensional simulations with a detailed transport model (blue curves), and one-dimensional simulations with a simplified transport model assuming a unity Lewis number (red curves).

by heat transfer (without the complications of detailed transport) anyway. These observations indicate that, under the present conditions, the transport processes primarily affect the local thermodynamic state without substantially altering the global ignition timing, whereas chemical kinetics remain the dominant factor governing ignition delay. A quantitative separation of chemical and transport contributions would require a dedicated sensitivity analysis, which will be addressed in future work.

This, however, is the observed behavior in the studied case ($\phi = 1$). Figure 7 shows the equivalence ratio alteration by thermo-diffusion for different initial equivalence ratio. For a mixture with initially $\phi = 9$, about 13% maximum equivalence ratio alteration can be observed. This shows that, for rich mixtures, the thermo-diffusion effect gets stronger. Under such conditions, the resulting local mixture inhomogeneity may be expected to exert a stronger influence on the ignition delay time and its interpretation, potentially contributing to discrepancies reported in the literature under nominally similar conditions.

Conclusions

This study investigates the impact of detailed transport on auto-ignition in an ammonia-hydrogen mixture for typical conditions of rapid compression machine (RCM) experiments by numerical simulations. The simulations model a laminar gas layer in the chamber of a RCM and incorporate detailed chemical kinetics and molecular transport processes, thus including effects of differential diffusion and unequal diffusivities of heat and species. Mixtures of ammonia/hydrogen with air are considered, in view of their projected significance as fuels for the future energy structure, and in view of the special character of hydrogen in respect to its molecular transport properties.

Results show how, in the fuel/mixture at compressed state, heat conduction to the cold wall creates an inhomogeneous temperature profile, with the maximum temperature occurring at the center, and a steep gradient at the cold wall. The

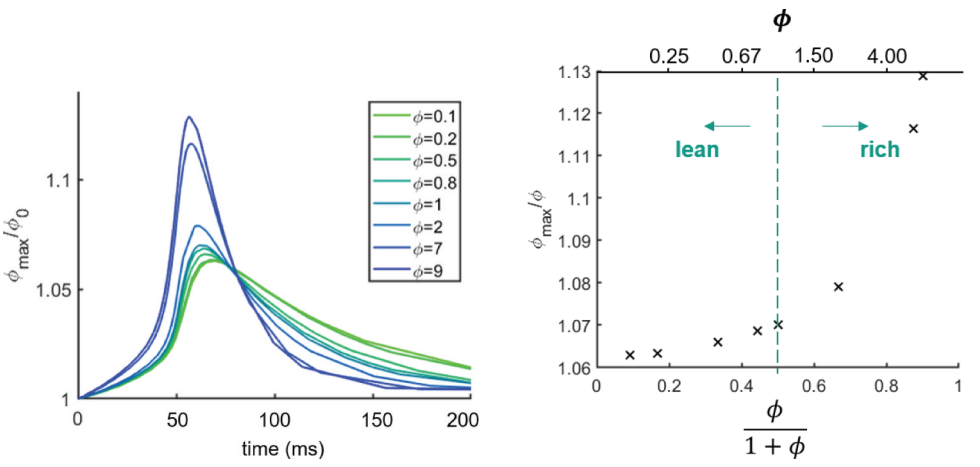

(a) Temporal Evolution

(b) Maximum alteration

Figure 7. Equivalence ratio alteration at different initial mixture equivalence ratios. Alteration of the mixture by thermo-diffusion already begins during compression, and builds up further within a span of about 60 ms, and then decays at longer times. The maximum alteration of ϕ can exceed 10%, and is most significant for rich mixtures.

inhomogeneous temperature profile, in turn, leads to an increasingly inhomogeneous mixture composition, driven by unequal diffusivities of species and of thermal energy. This can occur well before chemical reaction significantly alters the mixture composition.

The effect may introduce a bias in practical RCM measurements involving hydrogen as a fuel, when the observed auto-ignition event actually occurs in conditions (e.g., with respect to the equivalence ratio and the molar shares of different fuel components) that are different from the intended, "nominal" values of equivalence ratio and fuel composition in a multi-component fuel. For similar reasons, the effect may also pose a challenge to comparisons of IDTs from RCM experiments and modeling simulations for validating chemical kinetic mechanisms.

To assess the magnitude of the effect, further studies involving more details of the RCM compression process, the chamber size and geometry, initial mixture composition, compression pressure and temperature will be conducted. It will also be helpful to develop experimental methods capable of assessing the extent of the "unmixing" effect in an actual RCM-experiment.

Nomenclature

α	Geometry-dependent parameter
$c_{p,i}$	Specific isobaric heat capacity of species i
D_i^T	Thermal diffusion coefficient of species i
IDT	Ignition delay time
j_i^D	Diffusive mass flux due to concentration gradients
λ	Thermal conductivity
n_s	Number of species

p_c	Pressure at end of compression
r	Spatial coordinate
RCM	Rapid compression machine
t	Time
T	Temperature
T_w	Wall temperature
w_i	Mass fraction of species i
ω_i	Chemical source term of species i
ϕ_0	Nominal equivalence ratio
c_p	Specific isobaric heat capacity
D_i	Mass diffusivity of species i
h_i	Specific enthalpy of species i
j_i	Species mass flux
j_i^T	Mass flux due to thermo-diffusion
M_i	Molar mass of species i
p	Pressure
R	Universal gas constant
r_{out}	Coordinate of the outer boundary
ρ	Density
t_c	Time at end of compression
T_c	Temperature at end of compression
V_i	Diffusion velocity of species i
x_i	Mole fraction of species i
ϕ	Equivalence ratio
ψ	Lagrangian coordinate

Acknowledgements

The authors gratefully acknowledge financial support from the German Research Foundation (Deutsche Forschungsgemeinschaft, DFG) within the project DFG/MOST project MA 1205/32-1.

Disclosure statement

No potential conflict of interest was reported by the author(s).

Funding

The work was supported by the Deutsche Forschungsgemeinschaft.

References

Alnasif A et al. 2023. Evolution of ammonia reaction mechanisms and modeling parameters: A review. Appl Energy Combust Sci. 15:0 100175.

Bird RB, Stewart WE, Lightfoot EN. 2002. Transport phenomena. 2nd ed. John Wiley & Sons.

Cavalcanti MHC et al. 2024. Hydrogen in burners: Economic and environmental implications. Processes. 120(11):2434. https://doi.org/10.3390/pr12112434

D'Antuono G, Galloni E, Lanni D, Fontana G. 2024. A relationship for estimating the ignition delay of hydrogen-enriched ammonia-air mixtures. Engineered Sci. 28:0 1074.

Donohoe N et al. 2014. Ignition delay times, laminar flame speeds, and mechanism validation for natural gas/hydrogen blends at elevated pressures. Combust Flame. 1610(6):0 1432–1443. ISSN 0010-2180.https://doi.org/10.1016/j.combustflame.2013.12.005

Drost S et al. 2023. Numerical and experimental investigations of CH4/H2 mixtures: ignition delay times, laminar burning velocity and extinction limits. Energies. 160(6). ISSN 1996-1073. 2621. https://doi.org/10.3390/en16062621

Giacomazzi E et al. 2023. Hydrogen combustion: features and barriers to its exploitation in the energy transition. Energies. 16(20):0 7174. https://doi.org/10.3390/en16207174

Goldsborough SS, Banyon C, Mittal G. 2012. A computationally efficient, physics-based model for simulating heat loss during compression and the delay period in RCM experiments. Combust Flame. 1590(12):3476–3492. https://doi.org/10.1016/j.combustflame.2012.07.010

Goldsborough SS, Mittal G, Banyon C. 2013. Methodology to account for multi-stage ignition phenomena during simulations of RCM experiments. Proc Combust Inst. 340(1):0 685–693. https://doi.org/10.1016/j.proci.2012.05.094

Goyal T, Trivedi D, Samimi Abianeh O. 2018. Autoignition and flame spectroscopy of propane mixture in a rapid compression machine. Fuel. 233:56–67. ISSN 0016-2361. https://doi.org/10.1016/j.fuel.2018.06.022

Grogan KP, Goldsborough SS, Ihme M. 2015. Ignition regimes in rapid compression machines. Combust Flame. 162(8):3071–3080. https://doi.org/10.1016/j.combustflame.2015.03.020

He X et al. 2019. Auto-ignition kinetics of ammonia and ammonia/hydrogen mixtures at intermediate temperatures and high pressures. Combust Flame. 206:0 189–200. ISSN 0010–2180. https://doi.org/10.1016/j.combustflame.2019.04.050

Hirschfelder JO, Curtiss CF, Bird RB. 1964. Molecular theory of gases and liquids. John Wiley & Sons.

Huang Z. 2024. Fuel blend combustion for decarbonization. Proc Combust Inst. 400(1):105776. ISSN 1540-7489.

Kawka L et al. 2020. Comparison of detailed reaction mechanisms for homogeneous ammonia combustion. Z für Physikalische Chem. 234(7–9):1329–1357. https://doi.org/10.1515/zpch-2020-1649.

Li J, Shu G, Wang L, Wei H, Pan J. 2024. An experimental investigation on hydrogen jet ignition of ammonia: emphasis on reactivity stratification. Proc Combust Inst. 400(1):105328. ISSN 1540-7489.

Liao W, Wang Y, Chu Z, Tao C, Yang B. 2023. Chemical insights into the two-stage ignition behavior of NH3/H2 mixtures in an RCM. Combust Flame. 256:112985. ISSN 0010-2180. doi: https://doi.org/10.1016/j.combustflame.2023.112985

Maas U, Warnatz J. 1988. Ignition processes in hydrogen-oxygen mixtures. Combust Flame. 74(1):0 53–69. https://doi.org/10.1016/0010-2180(88)90086-7

Pan J et al. 2020 08. An experimental investigation on pre-ignition phenomena: emphasis on the role of turbulence. Proc Combust Inst. 38(4):5801–5810. https://doi.org/10.1016/j.proci.2020.06.240

Paul P, Warnatz J. 1998. A re-evaluation of the means used to calculate transport properties of reacting flows. Symp (Int) Combust. 270(1):495–504. ISSN 0082-0784. Twenty-Seventh Sysposium (International) on Combustion Volume One.https://doi.org/10.1016/S0082-0784(98)80439-6

Shrestha KP, Seidel L, Zeuch T, Mauss F. 2018. Detailed kinetic mechanism for the oxidation of ammonia including the formation and reduction of nitrogen oxides. Energy Fuels. 32 (10):10202–10217. https://doi.org/10.1021/acs.energyfuels.8b01056

Sung C-J, Curran HJ. 2014. Using rapid compression machines for chemical kinetics studies. Prog Energy Combust Sci. 44:1–18. https://doi.org/10.1016/j.pecs.2014.04.001

Warnatz J, Maas U, Dibble RW. 2006. Combustion: physical and chemical fundamentals, modeling and simulation, experiments, pollutant formation. 4th ed. Springer.

Wilson D, Allen C. 2017. A comparison of sensitivity metrics for two-stage ignition behavior in rapid compression machines. Fuel. 208:305–313. ISSN 0016-2361. https://doi.org/10.1016/j.fuel.2017.07.002

Wu C et al. 2024. Experimental and numerical investigation of the induced ignition process in ammonia/air and ammonia/hydrogen/air mixtures. Proc Combust Inst. 400(1):105466. ISSN 1540-7489.